100 GHZ SOI GAP WAVEGUIDES

S. Rahiminejad[1], A. Algaba Brazález[1], H. Raza.[1], E. Pucci[1], S. Haasl[2], P.-S. Kildal[1] and P. Enoksson[1]*

[1]Chalmers University of Technology, Gothenburg, Sweden
[2]Royal Institute of Technology, Stockholm, Sweden

ABSTRACT

Two gap waveguide technologies, groove and ridge, are presented here for F-band applications. Three different groove gap waveguide devices and four different ridge gap waveguide devices have been fabricated. All of them were micromachined to achieve the feature size required for the frequency band and fabricated in a single process using SOI wafers.

The two types provide a more robust coupling to standard waveguides and high frequency probes.

Measurements for most of the devices are shown in this paper, showing robust measurements and good agreement with simulations. More measurements need to be done but the initial ones show the promise both in the manufacturing technique and the coupling.

KEYWORDS

Gap Waveguide, Micromachining, Bed of nails, High-frequency, Waveguide, Groove, Ridge,

INTRODUCTION

Gap waveguides are a new type of waveguides for RF applications that allow a more robust assembly method compared to standard waveguides. Gap waveguides exist in three different varieties; ridge, groove and microstrip gap waveguides [1]. First presented for the 10-20 GHz range in 2011 [2], the technology has since then been used for filters [3], packaging of microstrip lines [4], microstrip filters [5] and also pin-flange adapters [6]. These devices have so far been manufactured by milling, and could be fabricated by milling due to their large structures. At higher operating frequencies (i.e. above 70 GHz), though, feature size prevents fabrication by conventional machining.

Simulations have shown the feasibility of two gap waveguide principles; the ridge gap waveguide and the groove gap waveguide. The principle of gap waveguides is based on realizing a stopband between two parallel plates, where one plate is a Perfect Electric Conductor (PEC) and the other a Perfect Magnetic Conductor (PMC). When these two surfaces are closer than λ/4 the wave cannot propagate between them. A PMC can be realized by periodic elements [7], in this case a bed of nails [8]. When a metal ridge or groove is embedded into the bed of nail surface (figure 1), two PECs are parallel to each other allowing the wave to propagate between these two surfaces. The wave is prohibited to propagate anywhere else due to the stopband between the PMC and the PEC. There is no need for conducting sidewalls, only a gap between the surfaces thereof the name gap waveguide.

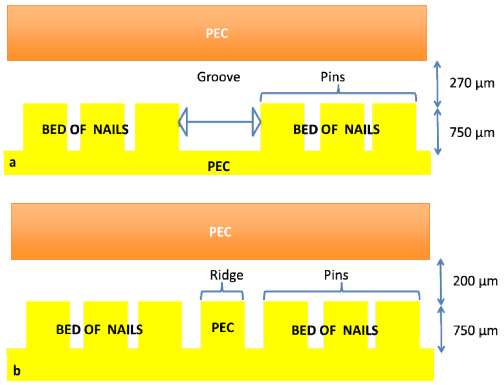

Figure 1: a) Groove gap waveguide b) Ridge gap waveguide

A ridge gap resonator and waveguide for 220-325 GHz were fabricated using MEMS technology and measured for the first time in 2012 [9]. The resonator was successfully measured and was used in order to verify losses. The ridge gap waveguide on the other hand, needed a transition structure for those frequencies, as seen in [10]. However this transition was highly sensitive to small gaps between it and the ridge. The transition to the standard rectangular waveguide interface is very sensitive to small misalignment gaps at those frequencies, and leakages occur even for gaps as small as 1-5 µm between the standard rectangular waveguide and the resonator. The issue of connecting to high-frequency gap waveguides needs to be addressed. In [6] an exterior solution is presented. The pin-flange adapter was designed to suppress leakage caused gaps between the measurement flange and any measurement object.

In this paper, we present the first ridge gap waveguides (r-GAP) for F-band and the first groove gap waveguides (g-GAP) for the same frequency range, fabricated by utilizing SOI wafers, thus achieving uniform height of the pins. Here the coupling is solved for the ridge gap waveguide by a microstrip-to-ridge gap waveguide transition. The groove gap waveguide has the benefit of not needing any transition structure to connect to a standard waveguide.

DESIGN

Two types of gap waveguides are presented; both fabricated using the same process and utilizing SOI wafers.

The first type is the groove gap waveguide. Three g-GAP devices have been fabricated: a straight g-GAP, a g-GAP with two 90° bends and a g-GAP resonator (figure 2a-c). The groove gap waveguides do not require specific coupling and are coupled with rectangular flanges. W-band flanges were used during measurement due to limited availability of the measuring equipment.

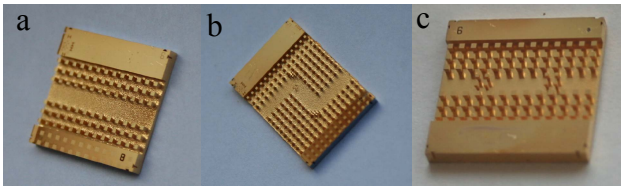

Figure 2: a) Straight groove gap waveguide, b) groove gap waveguide with two 90° bends, c) groove gap resonator.

The second type is the ridge gap waveguide. Four r-GAP devices were fabricated: a straight r-GAP, a 90° bend r-GAP, and two resonator types (Fig 3a-d). As coupling with ridge gap waveguides to standard flanges is extremely sensitive to misalignment gaps, a novel microstrip-to-ridge gap waveguide transition was used. That is why the ridge is completely surrounded by pins compared to the previous design of the ridge gap waveguide for 220-325 GHz [10]. The difference between the r-GAP resonators is how many pins there are between the resonance ridge and the transition structure, affecting the loose coupling to the resonator, marked with a red circle in figure 3c and 3d.

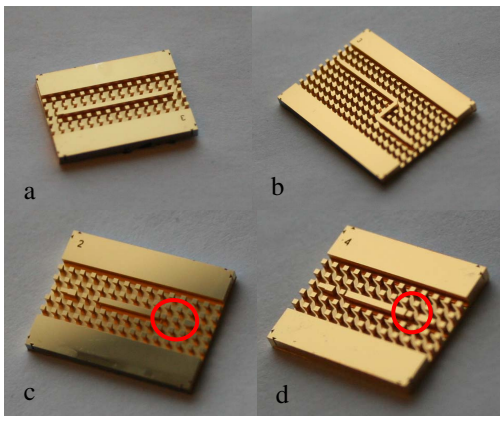

Figure 3: a) Straight ridge gap waveguide, b) ridge gap waveguide with two 90° bends, c) ridge gap resonator with two pin rows (marked with a red circle) between the ridge and the transition, d) ridge gap resonator with one pin row (marked with a red circle) between the ridge and the transition.

MICROSTRIP-TO-RIDGE GAP WAVEGUIDE TRANSITION DESIGN

A low-loss 127-µm thick alumina substrate is chosen with the following characteristics: $\varepsilon_r = 9.8$ and $\tan\delta = 0.0002$. Two 50 ohm input and output microstrip lines are added to feed the circuit. The center frequency of operation is 100 GHz.

The ridge has two λ/4 sections at each end of the ridge (one at the input and another one at the output) which cover the microstrip rectangular patch and couple the signal. This signal is guided along the central ridge section to the other side of the circuit.

Small coplanar pads were added at both sides of the input and output feeding microstrip line in order to be able to measure with the available probes. These coplanar pads located at both sides of the input/output microstrip line need to be grounded. Therefore, the design of vias has also been taken into account following the specifications from the PCB manufacturer, figure 4a.

The initial design of the transition is based on the overlapping of two λ/4 sections: one microstrip rectangular patch and a section of the r-GAP [10] , figure 4b. The matching was improved by optimizing the length and the width of the microstrip patch and the r-GAP λ/4 section.

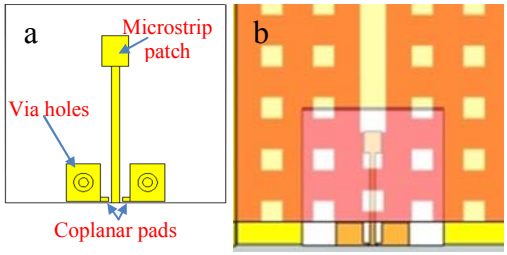

Figure 4: a) The microstrip transition and b) how the ridge will overlap the transition when being flipped on top of it.

The geometry contains two different interfaces: the r-GAP located upside down and the microstrip PCB which is placed in the opposing metal plate. The gap between the pins and the lower metal plate is 0.2 mm, see figure 5.

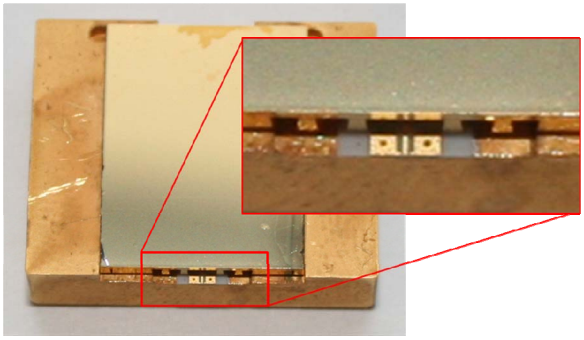

Figure 5: View of the microstrip-to-ridge gap waveguide transition. The chip is flipped upside down, facing the microstripline. The visual part of the microstripline is where the contact probes will connect.

FABRICATION

A 6" SOI wafer with a 750 µm device layer, 1.5 µm oxide layer and a 500 µm handling wafer was used. The wafer was sputtered with 1 µm Al that was used as a hard-mask. The large thickness was needed to sustain etching of 750 µm of Si. The Al was patterned with a 7-µm thick photoresist that was left on during etching.

DRIE was used to define the pins. The slope of the sidewalls on the pins varies depending on the width of the pins. The 450 µm wide pins had a slope average of 1:11, i.e. the base was 68 µm narrower than the top. The 300 µm wide pins had an average of 1:10 and the 150 µm wide pins had an average of 1:16. The most crucial slope

was for the 150 µm wide pins. Because the pins are 150 µm wide the slope of these pins needs to be larger than 1:10 otherwise the pin will etch off when etching down to 750 µm. The slope was achieved by tuning the etch and passivation time and the pressure. The slope is a benefit as it extends the bandwidth.

After DRIE the Al hard-mask was stripped. The wafer was diced into strips where each strip had devices of only one design. The strips were then sputtered with a seed layer and electroplated to achieve a 1 µm thick Au layer. The reason was to attain a conducting surface at these frequencies with a thickness larger than the skin depth. A cross section of the devices can be seen in figure 6.

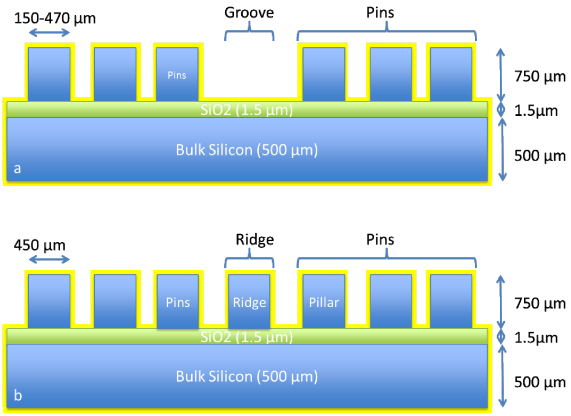

Figure 6: a) Groove gap waveguide cross section and dimensions. b) Ridge gap waveguide cross section and dimensions. (Not to scale)

RESULTS

Figure 7 shows simulated and measured results for the straight g-GAP. The simulated S11 is below -15 dB between 90-118 GHz and the measured S11 is below -10 dB for the same frequency range.

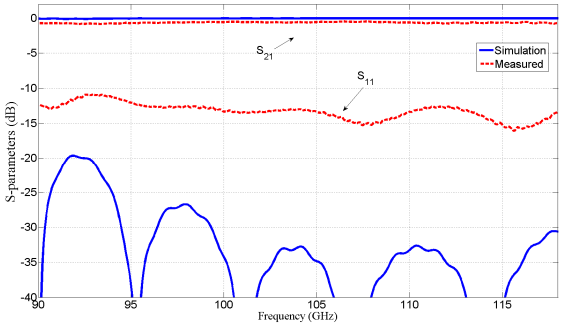

Figure 7: Simulated (solid blue line) and measured (dashed red line) S11 and S21 for the straight groove gap waveguide.

Figure 8 shows simulated and measured results for the g-GAP with two 90° bends. The return loss is below -15 dB between 100 and 118 GHz for measured data and below -20 dB for simulated data.

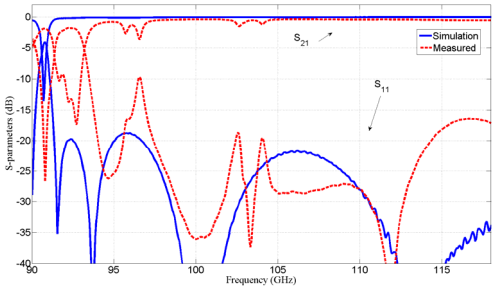

Figure 8: Simulated (solid blue line) and measured (dashed red line) S11 and S21 for the 90^{O} groove gap waveguide.

Figure 9 shows simulated and measured results for the g-GAP resonator with two resonance peaks. Table 1 shows simulated and measured Qs.

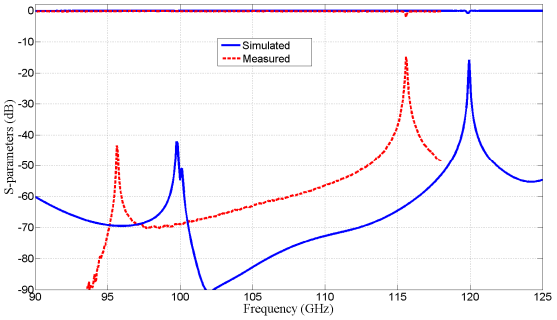

Figure 9: Simulated (solid blue line) and measured (dashed red line) S11 and S21 for the groove gap resonator with resonances at 95.64 GHz and 115.6 GHz and simulated at 99.75 GHz and 119.9 GHz

Table 1: Simulated and measured Qs and resonance frequencies for the g-GAP resonator

	Q1 (f1)	**Q2 (f2)**
Simulated	763.3 (99.75 GHz)	1998 (119.9 GHz)
Measured	1210 (95.64 GHz)	1156 (115.6 GHz)

Figure 10 represents the simulated circuit performance in terms of S-parameters for the straight ridge gap waveguide. The simulation result shows a S11 parameter better than -15 dB in 25.8% bandwidth, and a S21 parameter with value below -1.1 dB in the same range. Therefore, the corresponding loss for each transition is less than 0.55 dB.

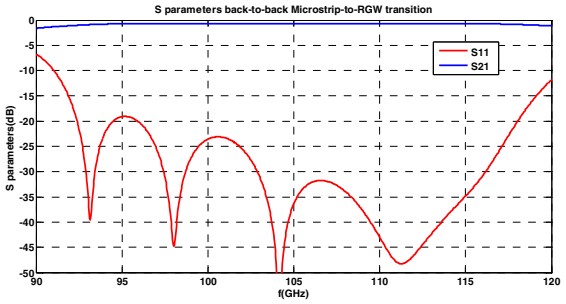

Figure 10: Computed S-parameters of two back-to-back microstrip-to-ridge gap waveguide transitions.

Measurements of the r-GAP resonator were performed and compared to simulations in Figure 11. Simulations of S21 give a resonance peak at 108.85 GHz with a Q-factor of 1168. In the measurement the resonance peak appear at 107.3 GHz with a Q-factor of 755.

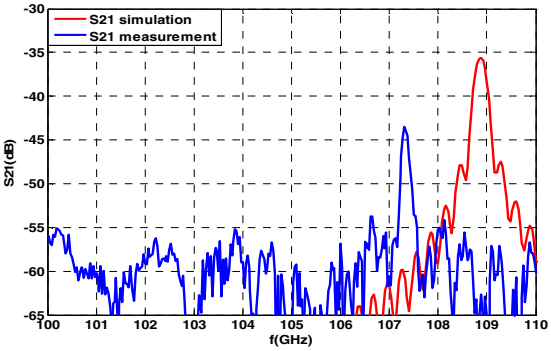

Figure 11: Computed and measured S-parameters of the ridge gap resonator with the microstrip-to-ridge gap waveguide transitions.

CONCLUSION

The straight g-GAP and the 90° g-GAP show a return loss below -20 dB during simulations and below -15 dB between 90-118 GHz and 100-118 GHz respectively, during measurement which is still a good performance. The resonator shows a shift of about 4 GHz compared to simulations. This could be due into the slopes of the pins, which has not been taken into account during simulations. The measured Q-values of the g-GAP resonator indicate low losses. The initial measurements on the r-GAP resonator correspond well with simulations. More measurements need to be done but these initial measurements show good indications of the coupling and gap waveguide technology. They also indicate a promising fabrication process.

ACKNOWLEDGEMENTS

This work has been supported by The Swedish Research Council VR, a project within then VINNOVA-funded Chase antenna systems VINN excellence center at Chalmers, Pakistan's NESCOM scholarship program, and Chalmers production area of advanced science for funding of the reported work. The authors are grateful to the nanofabrication laboratory at Chalmers University of Technology for their help in the fabrication process and to Mattias Ferndahl at the Microwave Electronics Laboratory for his support with the measurements.

REFERENCES

[1] P.-S. Kildal, "Three metamaterial-based gap waveguides between parallelmetal plates for mm/submm waves," in 3rd European Conference on Antennas and Propagation (EuCAP2009), Berlin, Germany, 2009.

[2] P.-S. Kildal, A. Uz Zaman, E. Rajo-Iglesias, E. Alfonso and A. Valero-Nogueira, "Design and experimental verification of ridge gap waveguides in bed of nails for parallel plate mode suppression", *IET Microwaves, Antennas & Propagation*, Vol.5, Iss.3, pp. 262-270, 2011.

[3] A. U. Zaman, A. Kishk, and P.-S. Kildal, "Narrow-band microwave filter using high Q groove gap waveguide resonators without sidewalls," IEEE Transactions on Components, Packaging and Manufacturing Technology, vol. 2, no. 11, pp. 1882–1889, 2012.

[4] E. Rajo-Iglesias, A. U. Zaman, and P.-S. Kildal, "Parallel plate cavity mode suppression in microstrip circuit packages using a lid of nails," IEEE Microwave and Wireless Components Letters, vol. 20, pp. 31–33, 2009.

[5] A. Algaba-Braz´alez, A. U. Zaman, and P.-S. Kildal, "Improved microstrip filters using PMC packaging by lid of nails," IEEE Transactions on Components, Packaging and Manufacturing Technology, vol. 2, no. 7, 2012.

[6] S. Rahiminejad, E. Pucci, S. Haasl and P. Enoksson, "Contactless pin-flange adapter for high-frequency measurements", 23rd Micromechanics and Microsystems Europe Workshop, September, 2012 Ilmenau, Germany.

[7] E. Rajo-Iglesias and P.-S. Kildal, "Numerical studies of bandwidth of parallel plate cut-off realized by bed of nails, corrugations and mushroom-type EBG for use in gap waveguides," IET Microw. Antennas Propag, vol. 5, pp. 282–289, March 2011.

[8] M. Silveirinha, C. Fernandes, and J. Costa. "Electromagnetic characterization of textured surfaces formed by metallic pins", IEEE Transactions on Antennas and Propagation, Vol 56, Iss 2, pp 405-415, 2008

[9] S. Rahiminejad, A.U. Zaman, E. Pucci, H. Raza, V. Vassilev, S. Haasl, P. Lundgren, P.-S. Kildal, and P. Enoksson. "Micromachined ridge gap waveguide and resonator for millimeter-wave applications" Sensors & Actuators A, 2012.

[10] S. Rahiminejad, A. U. Zaman, E. Pucci, H. Raza, V. Vassilev, S. Haasl, P. Lundgren, P.-S Kildal, P. Enoksson, "Design of Micromachined Ridge Gap Waveguides for Millimeter-Wave Applications" In Procedia Engineering, volume 25, pages 519–522, 2011.

[11] G. Strauss, W. Menzel, "Millimeter-Wave MMIC Interconnects Using Electromagnetic Field Coupling", 1994 IEEE 3rd Topical Meeting on Electrical Performance of Electronic Packaging, pp. 142-144, 1994.

CONTACT

*S. Rahiminejad, tel: + 46 (0)317721874; rahimine@chalmers.se